Pergamon

Geochimica et Cosmochimica Acta, Vol. 65, No. 1, pp. 47–62, 2001

0016-7037/01 $20.00 + .00

PII S0017-7037(00)00513-5

Partitioning of Sr^{2+} and Mg^{2+} into calcite under karst-analogue experimental conditions

YIMING HUANG and IAN J. FAIRCHILD*
School of Earth Sciences and Geography, Keele University, Staffordshire, ST 5 5BG, UK

(*Received March* 17, 2000; *accepted in revised form July* 10, 2000)

Abstract—There is a paucity of experimental data on calcite precipitation from waters at low ionic strength and low ratios of Mg/Ca and Sr/Ca, using controlled and constant precipitation rates. Such data are particularly needed for studies of speleothem geochemistry in relation to palaeoclimates.

We carried out a series of experiments using a karst-analogue set-up in a chamber of constant temperature and 100% humidity. A steady flow of $NaHCO_3$ and $CaCl_2$ solutions at PCO_2 around $10^{-3.2}$ were mixed just before passage through a tube (analogous to a soda-straw stalactite) and allowed to drip onto a surface, analogous to a stalagmite. Growth rates were comparable with linear extension rates of natural speleothems.

Analytical spots gave reproducible analyses in later analytical cycles after ablation of surface calcite with Na and Mg contamination. Different crystals from the same experiment tended to show positive covariation of Na and Mg with negative covariation with Sr. This may be due to the presence of growth hillocks with vicinal faces with differential partitioning behaviour.

The result for the partition coefficient for Mg (D_{Mg}) at 25°C is 0.031 ± 0.004, which is quantitatively in good agreement with the trends of previous workers. At 15°C, the result is 0.019 ± 0.003. The temperature dependency is higher than experimental data on seawater-analogue solutions, but lower than a previous estimate based on a comparison of speleothem chemistry with single water analyses.

Data for D_{Sr} are mainly in the range of 0.057 to 0.078, with a possible weak dependency on growth rate, consistent with previous experimental work. Absolute values are higher than studies in Mg-free saline solutions, which is attributed mainly to salinity effects. Values of D_{Sr} are nevertheless somewhat lower than in natural caves, which may relate to crystal growth factors.

Mg partition coefficient values should allow robust determination of solution Mg/Ca compositions in enclosed caves, which are at constant temperature on the decadal timescale. The inferred sensitivity of D_{Sr} to growth rate factors implies that Sr values should be interpreted more cautiously. Muted changes could relate entirely to growth rate variations, whereas changes of large magnitude imply a control by solution composition. The absence of local (tens of micron scale) antipathetic variations in Sr and Mg in studied natural speleothems, implies that intracrystalline zoning phenomena, if present, are on a finer scale in those natural materials compared with experimental products.

1. INTRODUCTION

Natural calcites contain measurable quantities of Mg and Sr, an observation that has generated an intense interest in the coprecipitation behaviour of these elements (Mucci and Morse, 1990; Morse and Bender, 1990). The ratio of trace element to calcium in solution is related to the same ratio in a homogeneous solid phase by use of a partition coefficient (D). For Mg, and likewise for Sr, $D_{Mg} = (Mg/Ca)_{calcite}/(Mg/Ca)_{solution}$. Partition coefficients have application to such issues as the conditions of precipitation of marine cements (e.g., Burton and Walter, 1991) and the modelling of meteoric and burial processes of carbonate diagenesis (e.g., Veizer, 1983; Banner, 1995). However, continued experimental studies have drawn attention to numerous variables that influence partitioning, so that the observed or effective partition coefficients cannot be regarded as thermodynamic quantities (cf. McIntyre, 1963) and so should only be used cautiously (Morse and Bender, 1990). A significant development is the growing understanding of the roles of growth mechanism on trace element incorporation (Paquette and Reeder, 1990; Paquette and Reeder, 1995). This leads to differing ion incorporation on different growth faces (Reeder and Grams, 1987) and on different sides of growth hillocks on rhombohedral faces (Staudt et al., 1994; Reeder, 1996). Growth hillocks display two different surface sites associated with the development of vicinal faces (that is, faces making a low angle to faces of a conventional crystal form). These discoveries emphasize that trace element incorporation is not an equilibrium process and also that the scale of analysis is a relevant factor. Nevertheless the observations of systematic behaviour of various ionic species at particular growth sites offer encouragement to the goal of quantitative prediction of partitioning behaviour.

Most of the literature focuses on marine or other saline systems, and much current work is being devoted to biologically-produced calcite and aragonite and an understanding of the vital effects that control partitioning (e.g., Nürnburg et al., 1996; Hart and Cohen, 1996; Xia et al., 1997). Ironically, the chemically simpler case of inorganic precipitation from solutions of low ionic strength (and lower Mg/Ca ratios) has been relatively neglected in experimental studies. This needs redress, given in particular the rapidly increasing interest in the use of cave precipitates (speleothems) for palaeoenvironmental studies. In freshwater karst environments, semicontinuous geochemical records of palaeoenvironments (or specifically palaeoclimates), have been generated from speleothems, at various time-resolutions. There has been particular emphasis on

*Author to whom correspondence should be addressed (i.j.fairchild@keele.ac.uk).

$\delta^{18}O$ and $\delta^{13}C$ (e.g., Bar-Matthews et al., 1999; McDermott et al., 1999), but with growing interest also in trace elements (e.g., Goede, 1994; Roberts et al., 1998; Ayalon et al., 1999; Huang et al., 2000), $^{87}Sr/^{86}Sr$ (e.g., Banner et al., 1996; Goede et al., 1998), and U-series isotopes (Kaufman et al., 1998). Numerous problems exist with the quantitative interpretation of the record, but these may be greatly reduced given an appropriate understanding of the source materials present and the geochemical processes acting at an individual site (e.g., Bar-Matthews et al., 1996; Fairchild et al., 2000). Recent work has emphasized the role of hydrology (influenced by the amount of rainfall) in controlling Mg/Ca and Sr/Ca ratios in cave waters from which the speleothems precipitated (Roberts et al., 1998; Fairchild et al., 2000). In turn this will lead to parallel changes in the Mg and Sr contents of speleothems, but modulated by precipitation conditions such as temperature and precipitation rates, the influence of which require experimental documentation.

Temperature variation is known to be a key control of Mg partitioning, whereas growth rate is unimportant (Mucci, 1987; Morse and Bender, 1990; Burton and Walter, 1991). Although temperatures are constant on decadal timescales in cave interiors, an understanding of possible temperature variations near a cave entrance became important in the study of Roberts et al. (1998) of Mg-variation of a Scottish speleothem. The Gascoyne (1983) comparison of waters and modern speleothems from different caves revealed much more pronounced temperature-related variation in D_{Mg} than expected from experimental studies (Oomori et al., 1987; Burton and Walter, 1991).

In the case of Sr, crystal growth rate has been demonstrated to be a crucial factor (Lorens, 1981; Teseriero and Pankow, 1996). Low and constant D_{Sr} values ($<<0.1$) were found to apply in the case of growth rates equivalent to a linear extension rate of speleothems of around 0.3 mm yr^{-1}, but D_{Sr} increased to over 0.1 given order-of-magnitude faster growth. The extension rate of 0.3 mm yr^{-1} is much higher than typical long-term growth rates of speleothems (e.g., McDermott et al., 1999) and similar to maximum rates up of to 0.5 mm yr^{-1} in active deposits in enclosed caves (e.g., Baker et al., 1998). However, estimates of D_{Sr} based on comparisons of waters with modern speleothems are all high: (0.13–0.2, bulk samples, Luray Caverns, Virginia, Holland et al., 1964; 0.13–0.23, Vancouver Island, and 0.09–0.30, Jamaica, bulk samples, Gascoyne, 1983; 0.15–0.16, microanalyses, northern Italy, Huang et al., 2000; 0.15, drilled sample of sectioned speleothem, Crag cave, western Ireland, our unpublished data). In the Italian site, annual laminae in the modern speleothems demonstrate that their annual extension rates are almost always less than 0.35 mm yr^{-1} (Huang et al., 2000). If the existing experimental data were to be appropriate for these settings, the implication would be that the speleothems only grew for a small proportion of the year, an awareness of which would be important for palaeoclimate studies.

The aims of this study are to determine appropriate partition coefficients for Sr and Mg at conditions analogous to natural caves, and their relationship with precipitation conditions such as precipitation rate and temperatures. This knowledge is an essential component of a strategy to retrieve palaeoclimate information from trace element variation in speleothems, but also contributes to a more general understanding of partitioning behaviour. The experimental set-up was designed to mimic the geometry, hydrodynamics, and low-ionic strength conditions encountered in natural karst caves and to precipitate calcite at typical rates of natural speleothems. To provide close control on solution composition, the solutions were prepared with a PCO_2 corresponding to that of the laboratory air rather than investigate the role of CO_2 degassing. Although degassing of karst waters seeping into caves is important, our measurements of natural cave dripwaters indicate that PCO_2 values are typically only $10^{0.1}$ to $10^{0.2}$ higher than cave atmospheres. To evaluate crystal chemistry on the same spatial scale as that used for high-resolution studies of natural speleothems (Roberts et al., 1998; Huang et al., 2000) we employed microanalytical (ion microprobe) techniques instead of the bulk analyses traditionally used.

2. EXPERIMENTAL AND ANALYTICAL CONDITIONS

The experimental apparatus is shown schematically in Figure 1. Separate $NaHCO_3$ and $CaCl_2$ solutions were made up from Puratronic Johnson Matthey reagents with concentrations of 0.007 to 0.0085 mol/L, and 0.0035 mol/L respectively. Aliquots of commercial standard solutions of Mg and/or Sr were added into $CaCl_2$ solutions and Mg/Ca and Sr/Ca molar ratios were fixed at 0.025 and 0.00023 respectively. The solutions were equilibrated with atmospheric PCO_2 by bubbling laboratory air overnight (PCO_2 was typically around $10^{-3.2}$). A peristaltic pump with multiple channels was employed for precise controllable solution delivery into one or two experimental cabinets which have a preset constant temperature (± 0.5°C) and 100% humidity maintained by open dishes of deionized water at the base of each cabinet. The solutions were allowed to equilibrate with the preset temperatures in the cabinet and then mixed at a Y-connector (fitted with a spiral thread to improve mixing). The mixed solution then passed through tubular growth sites (analogous to soda straw stalactites) and dripped several cm onto a solid convex "stalagmite" surface. The apparatus was checked daily; occasionally it was necessary to remove an air bubble in the Y-connector by temporarily detaching the tubing. The mixed solution had saturation index values (logarithm of ratio of ionic activity product to solubility product) with respect to calcite in the range of 0.75 to 1.15 (calculated using PHREEQM, Appelo et al., 1994). These were calculated using actual measurements of mixing ratio. These mixing ratios were close to the intended ratio of 1:1 (%$CaCl_2$ in the mixed solutions was between 48 and 52%, except for one case where it was 58%). Although these saturation index values are at the upper end of those encountered in caves, initial precipitation rates from thin films supersaturated with calcite depend less strongly on supersaturation than in agitated bulk solutions. Instead, they are a linear function of calcium concentration provided that the solution is replenished more often than approximately every 100 s (Buhmann and Dreybrodt, 1985; Baker et al., 1998). In our experiments, flow rates were 4.78 $\pm$ 0.22 mL hr^{-1} falling from the tube onto the surface as individual drops approximately 0.07 mL in volume, that is the time between drops averaged 68 s.

Early experiments were carried out using natural soda straw stalactites and incipient stalagmites from a disused limestones mine as substrates for new precipitates. However, it is difficult to obtain natural material with identical diameters and surface morphology. In addition, because natural straws are very fragile, they are difficult to connect to the experimental apparatus and to weigh the amount of precipitate. Therefore, in the main experiments reported here, glass tubes (0.4 mm diameter by 2 cm length) and plates (thin section glass, 2.5 $\times$ 2.5 cm) precoated with calcite precipitates were used. The seed precipitates were prepared using much more concentrated $NaHCO_3$ and $CaCl_2$ solutions (0.8 and 0.4 mol/L respectively). In our experiments, only an insignificant amount of spontaneous nucleation occurred; this was in the Y-connector. On the contrary, SEM images of the tubes and plates demonstrate that crystal overgrowth dominated: the calcite seeds are 3 to 6 μm rhombohedra (Fig. 2a), whereas the controlled experimental products are much larger rhombohedra (40–100 μm, Fig. 2b).

The mass of the precoated calcite on the plate was $\sim$0.034 g on average and on the straw was $\sim$0.014 g. The glass plates and straws

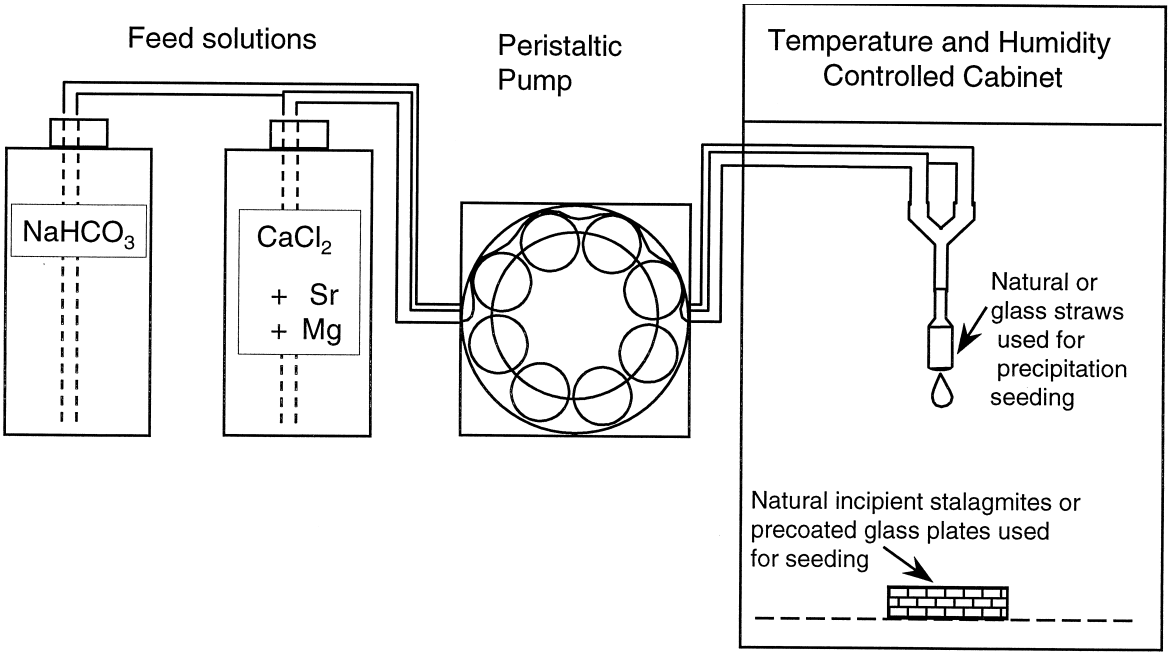

Fig. 1. Schematic diagram of experimental apparatus.

after calcite precipitation during the experiment were dried in an oven at 105°C overnight, then were weighed after equilibration at room temperature. The amount and rate of precipitation on each plate and straw was calculated and is presented in Table 1 together with temperature and supersaturation data. The loss of ions from each aliquot of solution was small (around 1% Ca loss for straws and 10% for plates, and the small effect on solution compositions has been corrected for in calculations (see Table 1).

The weight gain on plates and straws was converted into a growth rate per unit area by a geometrical model assumption based on Figure 2a. The glass was effectively completely covered by a mass of joined small crystals, with a 25% cover of clusters of slightly larger crystals. The effective surface area was conservatively estimated as 1.25 times the area of the glass plate (or tube) underlying the seeds. It is appropriate to use a conservative estimate because there is some evidence that effective surface area showed a moderate decrease during the experiments. Figure 3 presents results of three comparable experiments on three seeded glass straws: straw 40 was dried and weighed seven times in the 14 d experiment whereas straws 41 and 43 were weighed only at the end of the period. Straw 40 shows a diminishing rate of weight gain which can be attributed to a decrease in effective surface area caused by disturbance of crystal surfaces by repeated interruption and drying (hence the lower total weight gain compared with experiments 41 and 43). However, the initial rate in experiment 40 was 0.35 mg/d (after 2 d), 35% higher than the 0.26 mg/d mean rate of experiments 41 and 43. This suggests that growth rates of the latter diminished with time (dashed line), perhaps related to decreasing surface area as a result of crystal enlargement and/or localization of growth.

Minimum estimates of crystal growth rate are obtained by using the conservatively estimated initial surface area: they are 0.57 to 1.54 nmol $min^{-1}cm^{-2}$ in the straws and 0.72 to 1.83 nmol $min^{-1}cm^{-2}$ on the plates. These compare well with rates of 0.9 to 2.1 nmol $min^{-1}cm^{-2}$ calculated using the theoretical treatment of Buhmann and Dreybrodt (1985) as presented in Baker et al. (1998) for our solution compositions with a film thickness of 50 μm. This film thickness is regarded as representative for speleothems as a result of field measurements by Baker et al. (1998). However, it is accepted that surface roughness (Fig. 2b) makes the concept of an exact film thickness difficult to apply. For comparison, if one assumes a 100 μm film thickness, the calculated growth rates are around 30% higher than for a 50 μm film: this would imply that not all crystals were simultaneously active. In conclusion, the estimate of effective surface area as assumed above is probably reasonably representative of the mean active surface area for the duration of each experiment, but the uncertainty needs to be borne in mind when comparing with results of other studies.

There is a positive correlation between precipitation rates and saturation index (SI) for both plates ($r^2 = 0.71$) and straws ($r^2 = 0.58$), with plates tending to show somewhat higher precipitation rates (Table 1), although the two sets of data overlap. The cover of new crystal growth on plates was uniform, although was concentrated in the upper parts of the straws. Nevertheless, no correlation was found between spatial position in the straw and crystal composition.

Trace element analyses were made on polished embedded mounts of the experimental plates and straws by secondary ion mass spectrometry (SIMS), using a CAMECA IMS-4F, to obtain high spatial resolution, high precision and low detection limits for Sr. Measured trace elements were Na, Mg, Si, Ca and Sr, of which Si was used to monitor silicate contamination. Analyses were carried out using the isotope mode and measuring conditions were 20 nA primary beam with diameter of ~30 μm, 25 μm image field aperture. One spot per crystal was analyzed. Only secondary ions with high energy (75 $\pm$ 20 eV offset) were measured to minimise interference. Because of Ca in calcite, ~1.2 ppm of interference is calculated to be detectable on Sr, (^{44}Ca on ^{88}Sr peak). Twenty to forty cycles of data for each measurement were normally collected during which time the beam penetrated up to 5 μm into the crystal. OKA calcite, whose elemental composition is given in Roberts et al. (1998) was used to calibrate the elemental results for Mg and Sr, and NBS610 glass was used for Si and Na. Relative precision of the trace element measurements is associated with the beam intensities for each element. Typical measurement precisions in this study are 0.5%, 1.5 and 3% for Mg, Sr and Na, respectively when expressed in their ratios to the constant level of Ca in the samples.

3. RESULTS

It was necessary both to distinguish the primary seed crystals and surface contaminants from the genuine experimental results. An example of the procedures used is shown by plate 7, which is referred to as a blank, being precipitated from solution without addition of Sr and Mg. Fourteen measurements of

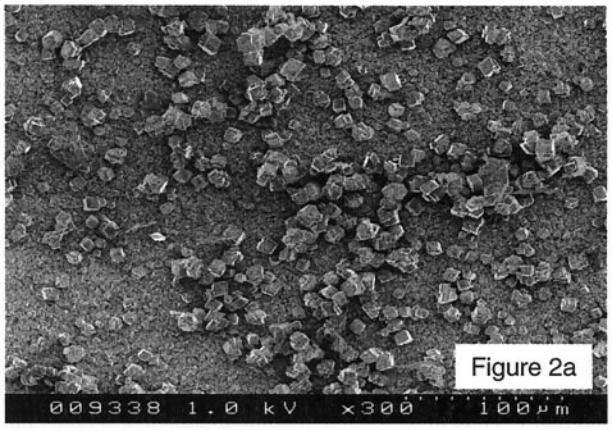

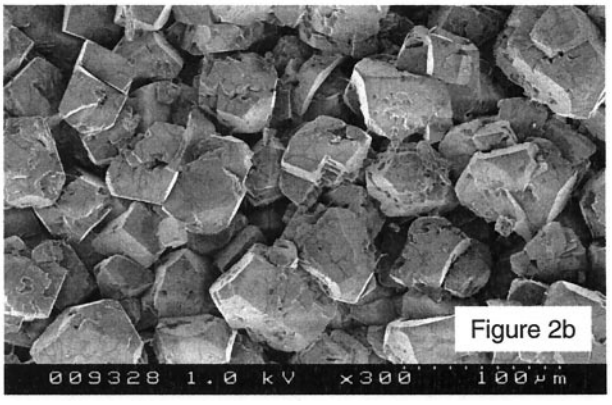

Fig. 2. SEM images of calcite precipitates; (a) seed crystals precipitated onto a glass plate. Note the complete coverage by very small crystals overlain by around 25% of slightly larger crystals; (b) experimental crystals from experiment 1. No differences in crystallography or crystal size were noted in products of different experiments.

different calcite crystals with 20 cycles for each measurement have been carried out (Figs. 4 to 6). It can be seen that the Na/Ca ratio (Fig. 4) is normally higher in early cycles of a measurement, then gradually decreases before reaches constant values. This is considered to be due to surface contamination during sample preparation and handling and accordingly only the later cycles of measurements with constant Na contents are likely to represent the real values in the samples. Two measurements with constant high Na/Ca ratio (4–6) are from crystals very close to the glass plate, which represents the seed calcite (individual crystals are small in relation to the 30 μm SIMS beam).

Sr data are presented in Figure 5. Leaving aside the high-Na seed crystals, Sr/Ca ratio is generally constant through the measurements, indicating that surface contamination has little effect on Sr results. In crystals where 1000*(Na/Ca) $<$ 0.9, there is a constant 1000*(Sr/Ca) value of around 0.005. Measurements from 5 experiments without added Sr (Table 1) show a very constant 1000*(Sr/Ca) ratio of 0.005 $\pm$ 0.0005, which represent both interference on Sr and experimental blank. We treat this as the effective total blank and it has been corrected for in Sr partition coefficient calculations.

Mg blank measurements presented by plate 7 are shown in Figure 6. Mg/Ca ratios mainly vary positively with Na/Ca ratio and decrease with time as the surface is removed by the ion beam. This indicates that Mg also is sensitive to surface contamination. Therefore only data from later cycles of a measurement (with constant Na value) are used for Mg results. At the low end of the trend, (Mg/Ca)*1000 is about 0.056 with (Na/Ca)*1000 ratios constant at about 0.9. The average of the 8 samples precipitated from solutions without added Mg added is 0.056 $\pm$0.017. This value is taken to represent the Mg/Ca experimental blank.

Using the above criteria, invalid measurements are excluded and Sr/Ca and Mg/Ca ratios of each measurement have been calculated by averaging the later cycles and the ratios of each sample were calculated from averages of measurements on different crystals. Generally one spot was analyzed per crystal. The values are listed in Table 1, including results from two experiments on natural seed materials, but the main discussion will focus on growths on seeded glass substrates.

The microanalytical approach of this study, in contrast to the bulk analyses normally used in previous studies, allows the heterogeneity of each sample precipitated under the same temperature to be examined. The use of an ion microprobe rather than electron microprobe also allows precise determinations of Mg, Sr and Na even at the low concentrations present in these experimental products. Mg/Ca and Na/Ca ratios of the different measurements of each sample calculated from the different cycles are presented in Figure 7. It can be seen that five of the nine samples (Plate 4, 9, 11 and Straw 44, 46 and 49) show a statistically significant correlation between Mg/Ca and Na/Ca in different measurements of a sample. When Sr/Ca is plotted against Na/Ca (Fig. 8), most samples exhibit negative correlation**,** although only three of these are statistically significant. In the smaller subset of the samples precipitated from solutions to which both Sr and Mg were added a negative correlation between Sr/Ca and Mg/Ca can be seen (Fig. 9). This is statistically significant in all cases except for Plate 6, which has much less variation in both Sr/Ca and Mg/Ca ratios than the other samples. All these variations are distinct from those of outer cycles ascribed to surface contamination.

4. DISCUSSION

4.1. Causes of Heterogeneity

In this section we examine potential causes (both experimental and crystallographic) of the heterogeneity of the microanalyses of the experimental product. Regarding experimental conditions, we note that the data from the straws show more variation for both Mg/Ca and Na/Ca than from the plates. For example, Straw 46 has much higher standard deviation in both Mg/Ca and Na/Ca than Plate 3, which is feed by solution from Straw 46. Hence one possible cause of heterogeneity are changes in solution composition related to incomplete mixing in the Y-connector. Such an effect would not influence solution Mg/Ca or Sr/Ca ratios, but would influence supersaturation and solution Na/Ca ratios. However large deviations from the in-

Table 1. Summary of experiments. The duration of each experiment was 48.7 days, except for the Pre-1 and -2 (experiments on natural seed materials), which were 45.8 days. The calcium precipitated in the straws has been allowed for when calculating results for the plates.

Experiment	**Pre-1**	**Pre-2**	**1**	**2**	**3**	**4**	**5**	**6**	**7**	**8**	**9**	**10**	**11**	**12**	**13**	**14**
Flow rate (ml day^{-1})	123.4	131.5	115.6	112.4	113.1	116.3	110.7	112.1	126.1	118.1	112.5	114.7	115.1	107.9	108.2	125.1
Temperature (°C)	15	15	25	25	25	25	25	25	25	25	15	15	15	15	15	15
(Mg/Ca)*1000 (solution)	12.4		25		25	25		25			25		25	25		
(Sr/Ca)*1000 (solution)		5.46		0.23	0.23		0.23	0.23				0.23	0.23		0.23	
Straw Number	**11**	**13**	**44**	**45**	**46**	**47**	**48**	**49**	**50**	**51**	**52**	**53**	**54**	**55**	**56**	**57**
Growth rate: mmol day^{-1}			0.0046	0.0051	0.0059	0.0041	0.005	0.0042	0.0057	0.0041	0.0033	0.0022	0.0037	0.0038	0.0037	0.0029
Growth rate: nmol cm^{-2} min^{-1}	1.09*	0.85*	1.2	1.33	1.54	1.07	1.3	1.09	1.48	1.07	0.86	0.57	0.96	0.99	0.96	0.75
Calcite saturation index	0.998	0.932	1.17	1.18	1.15	1.08	1.09	1.04	1.24	1.13	1.04	1	1.01	1.04	1.06	1.1
% Ca precipitated	1**	1**	2.3	2.6	3	2	2.6	2.1	2.6	2	1.7	1.1	1.8	2	2	1.3
1000*(Na/Ca)			0.49	0.94	0.44	0.22	0.32	0.46			0.40	0.98		0.22		
(standard deviation of above)			0.26	0.30	0.17	0.04	0.12	0.31			0.08	0.04		0.10		
1000* (Mg/Ca)	0.46		0.95	0.03	0.75	0.69	0.05	1.00			0.42	0.08		0.54		
(standard deviation of above)			0.25	0.00	0.17	0.02	0.02	0.12			0.05	0.02		0.08		
1000*(Sr/Ca)		0.4765	0.0049	0.0191	0.0307	0.0048	0.0237	0.0183			0.0062	0.0205		0.0051		
(standard deviation of above)			0.0006	0.0021	0.0057	0.0004	0.0043	0.0025			0.0007	0.0004		0.0002		
D_{Mg}	0.022		0.036		0.027	0.025		0.038			0.014			0.019		
D_{Sr}		0.077		0.061	0.111		0.081	0.057				0.067				
Plate Number	**STG3**	**STG5**	**1**	**2**	**3**	**4**	**5**	**6**	**7**	**8**	**9**	**10**	**11**	**12**		**13**
Growth rate: mmol day^{-1}			0.0202	0.02	0.0196	0.0164	0.016	0.0157	0.0206	0.0166	0.0125	0.0081	0.0116	0.0097		0.0091
Growth rate: nmol cm^{-2} min^{-1}	1.07*	0.66*	1.8	1.78	1.74	1.46	1.42	1.4	1.83	1.48	1.11	0.72	1.03	0.86		0.81
Calcite saturation index	0.995	0.929	1.16	1.18	1.14	1.07	1.08	1.03	1.2	1.13	1.03	1	1.01	1.03		1.08
% Ca precipitated			10	10.2	9.9	8.1	8.3	8	9.3	8	6.3	4	5.8	5.1		4.2
Final calcite saturation index			1.13	1.15	1.11	1.05	1.06	1.01	1.18	1.11	1.02	0.99	0.99	1.02		1.072
1000*(Na/Ca)			0.48	0.36	0.41	0.23	0.52	0.65	0.47		0.60	0.54	0.50	0.58	0.47	
(standard deviation of above)			0.20	0.22	0.20	0.07	0.26	0.07	0.25		0.23	0.23	0.22	0.07	0.19	
1000*(Mg/Ca)	0.47		0.91	0.05	0.87	0.82	0.05	0.83	0.06		0.54	0.07	0.47	0.60	0.06	
(standard deviation of above)			0.14	0.05	0.16	0.06	0.01	0.06	0.04		0.06	0.05	0.06	0.05	0.04	
1000*(Sr/Ca)		0.4349	0.0047	0.0237	0.0236	0.0044	0.0235	0.0218	0.0046		0.0049	0.0212	0.0236	0.0049	0.0052	
(standard deviation of above)			0.0003	0.0026	0.0024	0.0001	0.0024	0.0013	0.0003		0.0004	0.0007	0.0031	0.0003	0.0003	
D_{Mg}	0.022		0.033		0.031	0.030		0.030			0.019		0.016	0.022		
D_{sr}		0.068		0.077	0.077		0.077	0.071				0.069	0.079			

* Precipitation rates were calculated using the relationship between precipitation rates and calcite saturation index from the pre-coated glass straws and plates.
** Amount of the precipitation was assumed.

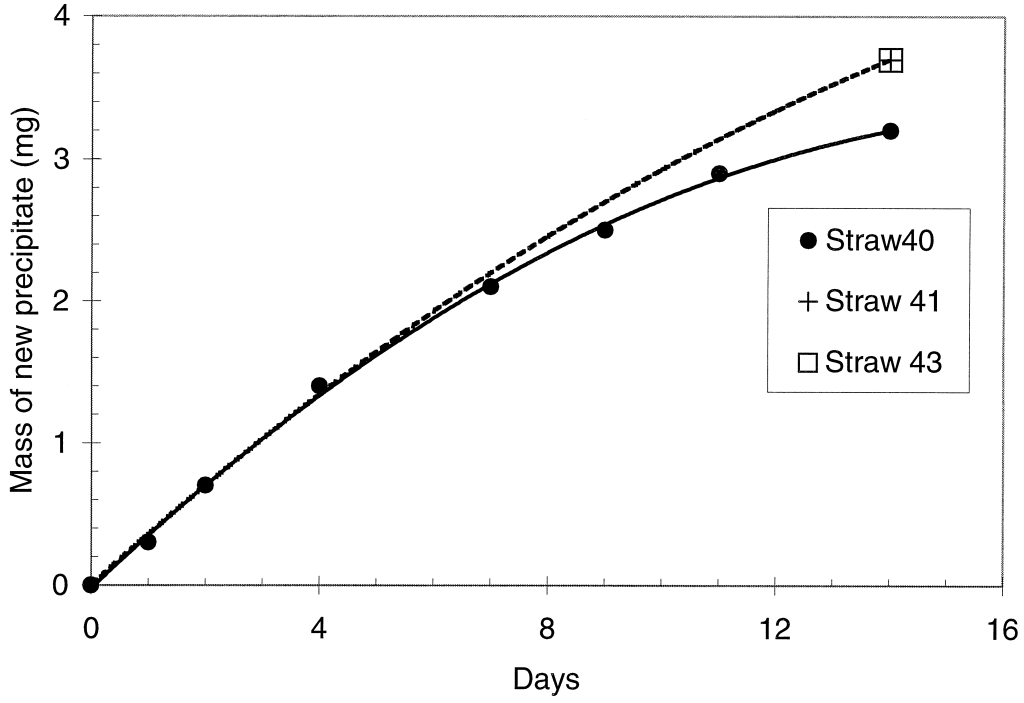

Fig. 3. Comparative study of weight gain in three 14 d experiments, in one of which the material was repeatedly dried and weighed. See text for discussion.

tended mixing ratio of the 50:50 would be needed to influence supersaturation significantly and measurements showed that the $\%CaCl_2$ in the mixed solution was in the range 48 to 52%, apart from one case where it was 58%. The required changes in growth rate to explain the Sr variations are outside the range of possible forcing by varying supersaturations. In addition, variation of precipitation rates also cannot explain the general negative correlation between Mg and Sr in experiment samples because Mg incorporation is independent of precipitation rates (Morse and Bender, 1990). Thus, it appears that variation of precipitation rates in a sample caused by inhomogeneous solutions should not be the major factor responsible for the change of Sr/Ca and Mg/Ca in a sample.

The positive covariation of Na with Mg and the negative covariation with Sr might suggest a causal relationship. Sodium is thought to substitute primarily in defect sites (Ishikawa and Ichikuni, 1984; Busenburg and Plummer, 1985). Defect sites might be more abundant in cases where lattice strain is increased by the substitution of the small Mg ion for Ca. However, it should be remembered that all these species are only present in trace quantities in our experimental products, and so lattice strain effects should be minimal. Alternatively, since Na incorporation has been found to relate to crystal growth rate (Busenburg and Plummer, 1985), its abundance might simply reflect the abundance of defects related to the local speed of crystal growth. However, this does not account either for the positive relationship with Mg or the negative one with Sr.

More specific relationships of variation of trace element abundance to growth mechanism are provided by experimental studies of zoned calcites. Reeder and Grams (1987) demonstrated trace element sector zoning in diagenetic calcite crystals in which Sr, Mn and Mg varied by ~50%, 85% and 95%, respectively between different growth sectors corresponding to at least three different crystallographic forms. This is unlikely to be relevant to our material because of the dominance of the single rhombohedral $\{10\bar{1}4\}$ crystallographic form (Fig. 2b). Also there was a positive covariation of Sr and Mg in the example of Reeder and Grams (1987). A more pertinent observation is that of Paquette and Reeder (1990) who found that trace element (Sr, Mg, Mn) zoning matched boundaries of vicinal faces of hillocks on calcite crystal surface {1014}. This phenomenon which they termed intrasectoral zoning has so far only been documented for this crystallographic form (e.g., Reeder, 1996; Reeder et al., 1999). The hillocks are considered to form by spiral growth on the growth surface around a presumed dislocation (Reeder, 1996). Paquette and Reeder (1990), Paquette and Reeder (1995) proposed that during growth certain trace elements showed a preferential tendency to partition into certain steps. These steps correspond to growth sites of differing geometry, hence influencing the relative coordination of ions of different size or other properties. Their data show that the vicinal faces with higher Mg content have lower Sr content. The Mg (and Mn) partitioning varied by typically a factor of 3 to 4, whereas for Sr it was more usually 1.2 to 1.4 (up to 2). In our data too, Mg shows the larger relative change. It is also implied from our data that Na incorporation is also related to these growth sites, which is not an obvious prediction from previous work given the monovalence of sodium. Quantitative differences between intrasectoral zones may depend on the precise geometry of the hillocks, e.g., Paquette and Reeder (1995) noted that the microtopography on $\{10\bar{1}4\}$ is sensitive to the supersaturation and the ratio of Ca^{2+}:CO_3^{2-}.

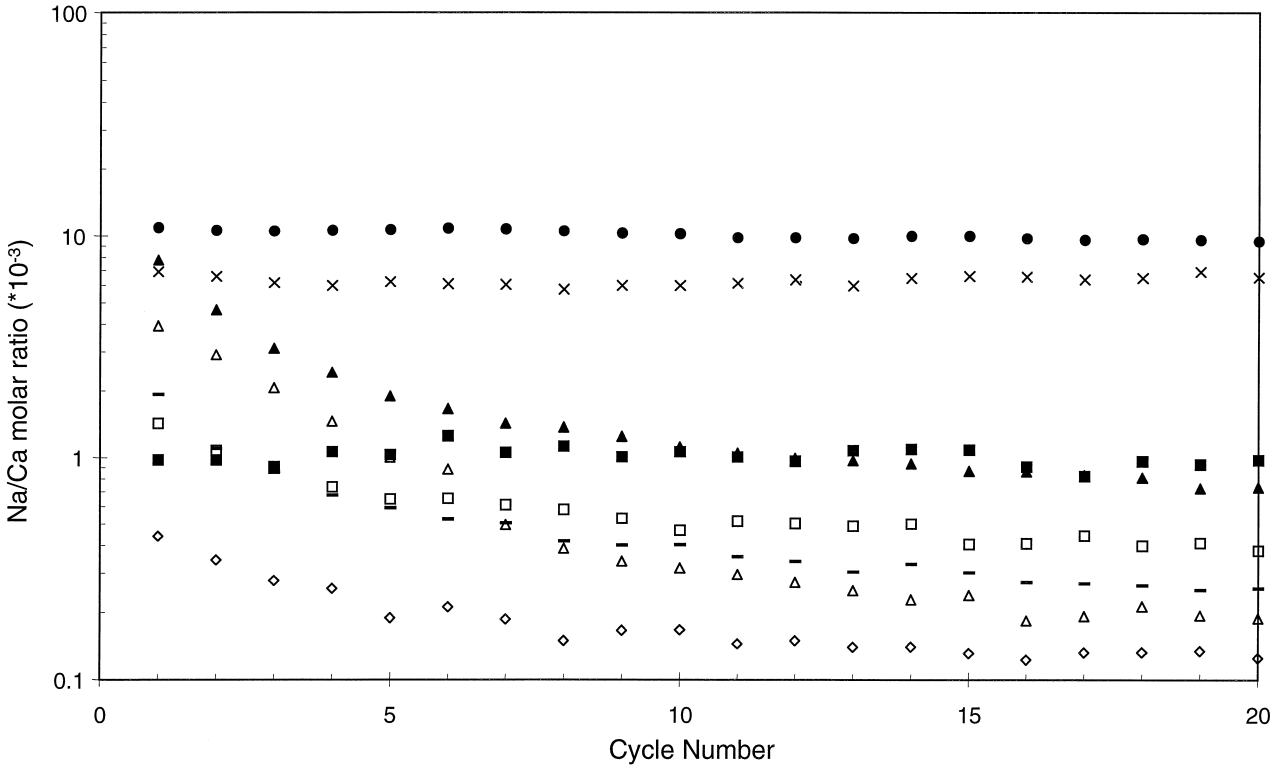

Fig. 4. Na measurements (expressed as Na/Ca) on successive cycles on the same analytical spot from each of several crystals from a blank experiment in which no Sr or Mg was added (experiment 7). Each symbol refers to a given crystal. Na gradually decreases and stabilized with successive cycles; this is considered to reflect the effect of removal of surface contamination. Two sets of points have constantly high Na contents and represent seed crystals.

The intrasectoral zonation mechanism is the only specific one known to us that can account for the observed differences between different analytical spots on crystals produced from a given experiment. Depending on the growth technique, such hillocks are known to occur on both smaller and larger scales (Teng et al., 1999; Paquette and Reeder, 1995). An implication of the dispersion of our analyses is that the size of the putative growth hillocks is on a scale approaching the size of the analytical spots on the ion microprobe (25 μm). Averaging of several crystals is necessary to derive the mean composition of such growth surfaces for comparison with previous partitioning studies where bulk analyses have been undertaken.

4.2. Controls on Sr partitioning

In Figure 10 we plot our D_{Sr} results, averaged over several crystals as indicated above, against crystal growth rate. The new data are compared with previous experimental studies that have identified growth rate as a key variable influencing D_{Sr}. In the following discussion we examine first the reasons for differences in D_{Sr} at a given rate before examining the rate relationship itself. Other influencing factors examined by previous workers are temperature, and aqueous Sr/Ca ratio, Na content and Mg/Ca ratio.

No perceptible influence of temperature on Sr partitioning was found in the temperature range of 40 to 98°C by Katz et al. (1972), although Malone and Baker (1999) documented a variation of D_{Sr} from 0.046 to 0.068 in the range 40°C to 200°C. Even if this genuinely reflects temperature rather than reaction rate (Shiraki and Brantley, 1995) the gradient of D_{Sr} of $0.00014°C^{-1}$ is too small to be checked within the range of temperatures of interest in the current work.

Pingitore and Eastman (1986), in agreement with Katz et al. (1972), found consistently low values of D_{Sr}, irrespective of other parameters, where values of solution Sr/Ca were relatively high (>0.004), compared with other experiments where it was kept at 0.001. However, such Sr/Ca ratios are much higher than considered in our experiments, or those of Lorens (1981), or typical ancient carbonate aquifers (Fairchild et al., 2000). This factor could account for the discrepancy between the experiments of Lorens (1981) where Sr/Ca was kept at 0.00003 and those of Tesoriero and Pankow (1996) where the ratio was 0.0055 to 0.117. This factor requires more experimental documentation for high-Sr aquifers (e.g., Banner, 1995; Roberts et al., 1998).

A strong influence of Na content (or salinity) was suggested by the work of Pingitore and Eastman (1986) who carried out comparative experiments with solutions containing 0.48 mol/L NaCl and no NaCl. Although the absolute precipitation rates were not controlled in their experiments, they found that the Na-rich solutions generated much lower values of D_{Sr} for both "normal" and "fast" (forced degassing) experiments. They suggested that Na out-competed Sr for non-lattice sites, confining Sr incorporation to the lattice Ca sites identified by Pingitore et

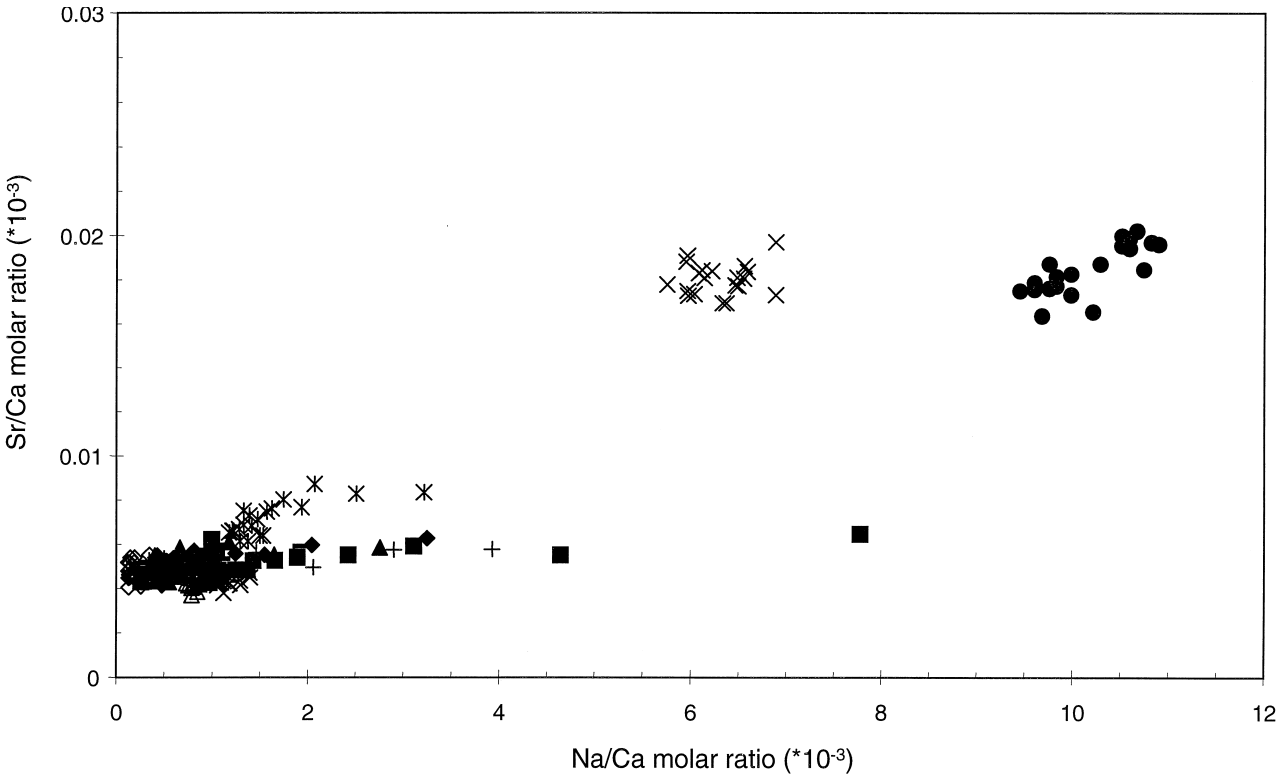

Fig. 5. Sr measurements, expressed as Sr/Ca, plotted against the Na/Ca (data from the same blank experiment as in Fig. 4. In contrast to the Na measurements, Sr contents did not show a significant variation through successive measurement cycles. This appears to indicate that Sr is not very sensitive to surface contamination. Two seed crystals, with higher Sr contents and Na contents, are distinguishable from most of the other measurements with 1000*(Sr/Ca) ratio ~ 0.005. (See Fig. 6 for the key of symbols).

al. (1992). We suggest this as a possible cause for the higher values of D_{Sr} obtained in our experiments in comparison with the results of Lorens (1981) and Tesoriero and Pankow (1996) (Fig. 10) who respectively used solutions with 0.69 M and 0.22 M NaCl. Our mixed solutions contained 0.0042 mol/L and 0.0035 M (corresponding to 96 and 80 mg L^{-1}), much closer to typical cave water compositions (e.g., Fairchild et al., 2000).

Mucci and Morse (1983) documented a clear dependence of D_{Sr} on the solution Mg/Ca ratio, in experimental precipitates of variably magnesian calcites, from marine-analog solutions with a range of Mg/Ca ratios from 1 to 5. Their data for Mg/Ca = 1 are illustrated in Figure 10: D_{Sr} has a range of 0.15 to 0.22 (whereas it is 0.3 at a Mg/Ca ratio of 5). They speculated that there was a coupled precipitation mechanism whereby larger ion size of Sr may compensate for the distortion caused by smaller ion size of Mg incorporated into calcite (see also Morse and Bender, 1990). However, this mechanism, which is disputed by Tesoriero and Pankow (1996), seems unlikely to be able to account for the relatively high value of D_{Sr} from Ernesto cave in relation to our new experiments as the solution molar Mg/Ca ratio at Ernesto is only 0.2 (Fairchild et al., 2000).

The growth rate-dependence of D_{Sr} (Fig. 10) is shown by the data of Mucci and Morse (1983), as explicitly discussed by Mucci, (1986), Lorens (1981) and Tesoriero and Pankow (1996). Our data display a weak correlation between D_{Sr} and precipitation rate with a slope of 0.015 ($r^2 = 0.16$). Although, this is not statistically significant, it is consistent with these relationships. An increase in Sr incorporation with increasing growth rate is not unexpected since all partition coefficients tend towards unity at high rates (Morse and Bender, 1990). For example a complete range of D_{Sr} and D_{Mg} up to unity are shown by calcite-dominated carbonate precipitates induced by freezing in which extremely rapid growth occurs in microenvironments adjacent to CO_2-rich gas bubbles (Fairchild et al., 1996; Killawee et al., 1998). However, the range of rates over which a rate-dependence occurs for a given ionic species will depend on the growth mechanisms and abundance and types of defect developed during growth. It follows that the absolute value of D_{Sr} at a given growth rate will also be partly dependent on crystal growth mechanisms. Any model related to growth mechanism may well depend on ionic strength, and our experiments are the only ones on Sr partitioning conducted at low ionic strengths in which growth rate has been controlled. Our values are significantly closer to those deduced from a low-Mg, low-Sr cave environment (Fig. 10; Huang et al., 2000) than previous experiments on low Mg/Ca ratio (but high Na) solutions (Lorens, 1981 and Tesoriero and Pankow, 1996), but differences remain. Although it is conceivable that there could be effects from the minor differences between the Na content of our solutions and those in the cave or other solution parameters, a difference in detailed growth mechanism is the most likely cause of the remaining discrepancy.

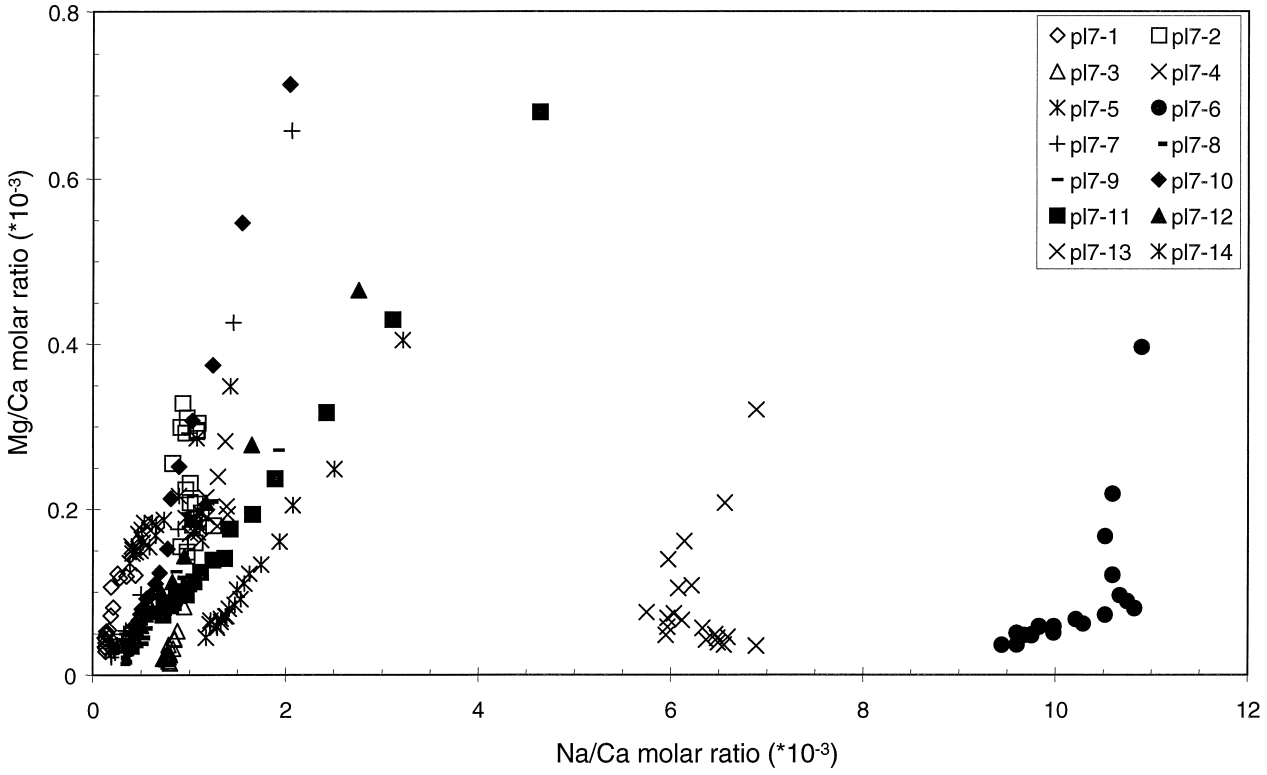

Fig. 6. Mg measurements expressed as Mg/Ca, plotted against Mg/Ca, plotted against the Na/Ca (data from the same blank experiment as in Fig. 4. Mg measurements show a strong covariation with Na, i.e., higher in early cycles and decreases with time. This suggests that, unlike Sr, Mg is very sensitive to surface contamination. The last few cycles yield a relatively constant 1000*(Mg/Ca) ratio of ~0.056.

4.3. Controls on Mg Partitioning

Previous studies have concluded that the controlling influences on D_{Mg} are temperature (Mucci, 1987; Oomori et al., 1987, Burton and Walter, 1991), Mg/Ca ratio (Mucci and Morse, 1983), salinity and/or sulphate content (Zhong and Mucci, 1989), and possibly PCO_2 (Burton and Walter, 1991; Hartley and Mucci, 1996), in addition to partitioning between sectoral or intrasectoral zones (Paquette and Reeder, 1995). Fig. 11 illustrates the variation in D_{Mg} with temperature based on data from a range of experimental studies (Howson et al., 1987; Oomori et al., 1987; Mucci, 1987; Burton and Walter, 1991; Hartley and Mucci, 1996) and field data from caves (Gascoyne, 1983; Huang et al., 2000). The data illustrate a positive correlation with temperature, but the role of factors other than temperature needs to be elucidated, particularly when comparing sea water-analog experiments with our own low ionic strength, low Mg/Ca ratio solutions.

Seawater has a molar Mg/Ca ratio of 5.1 and precipitates calcite with 8 to 12 mol% $MgCO_3$. This high Mg content is far removed from the idealized conditions under which thermodynamic theory predicts constant partition coefficient values (McIntyre, 1963). Therefore variations of D_{Mg} with Mg/Ca are not unexpected: indeed it is surprising how little change in D_{Mg} is demonstrated across a wide range of Mg/Ca. Mucci and Morse (1983) demonstrate an increase in D_{Mg} from 0.017 $\pm$ 0.002 to 0.027 as Mg/Ca falls to unity in artificial seawater solutions. Additionally, Zhong and Mucci (1989) and Burton and Walter (1991) demonstrated a small increase in D_{Mg} (of around 0.004–0.006) with decreasing salinity which they attributed largely to sulphate content rather than salinity per se. There is an excellent agreement of these trends both with the low ionic strength experiments of Howson et al. (1987), who found D_{Mg} values to be constant at around 0.030 $\pm$ 0.005 at a range of Mg/Ca values up to unity, and our own mean value of 0.031 $\pm$ 0.004. The different PCO_2 values used by us and by Howson et al. (1987); (see also House et al., 1988) bracket the typical values found in caves. Also, the lack of significant difference in D_{Mg} is consistent with the experimental work of Hartley and Mucci (1996) on marine-analog solutions in which no relationship to PCO_2 was found. There is a discrepancy with the lower D_{Mg} value obtained by Oomori et al. (1987), but these authors used uncontrolled growth by homogeneous nucleation which it is argued could generate metastable precipitates which may readily recrystallize (Howson et al., 1987; Hartley and Mucci, 1986).

Having established a congruence of our work with other experimental data, the temperature variation can now be reassessed. Our work shows a drop in D_{Mg} to 0.019 $\pm$ 0.003 at 15°C (Fig. 11) which suggests that an intermediate response to temperature is represented between the high sensitivity suggested by Gascoyne (1983) in his reconnaissance study and the lower sensitivity of marine-analog experimental solutions (Burton and Walter, 1991). All data converge at lower temperatures where the data most comparable with our experiments are the

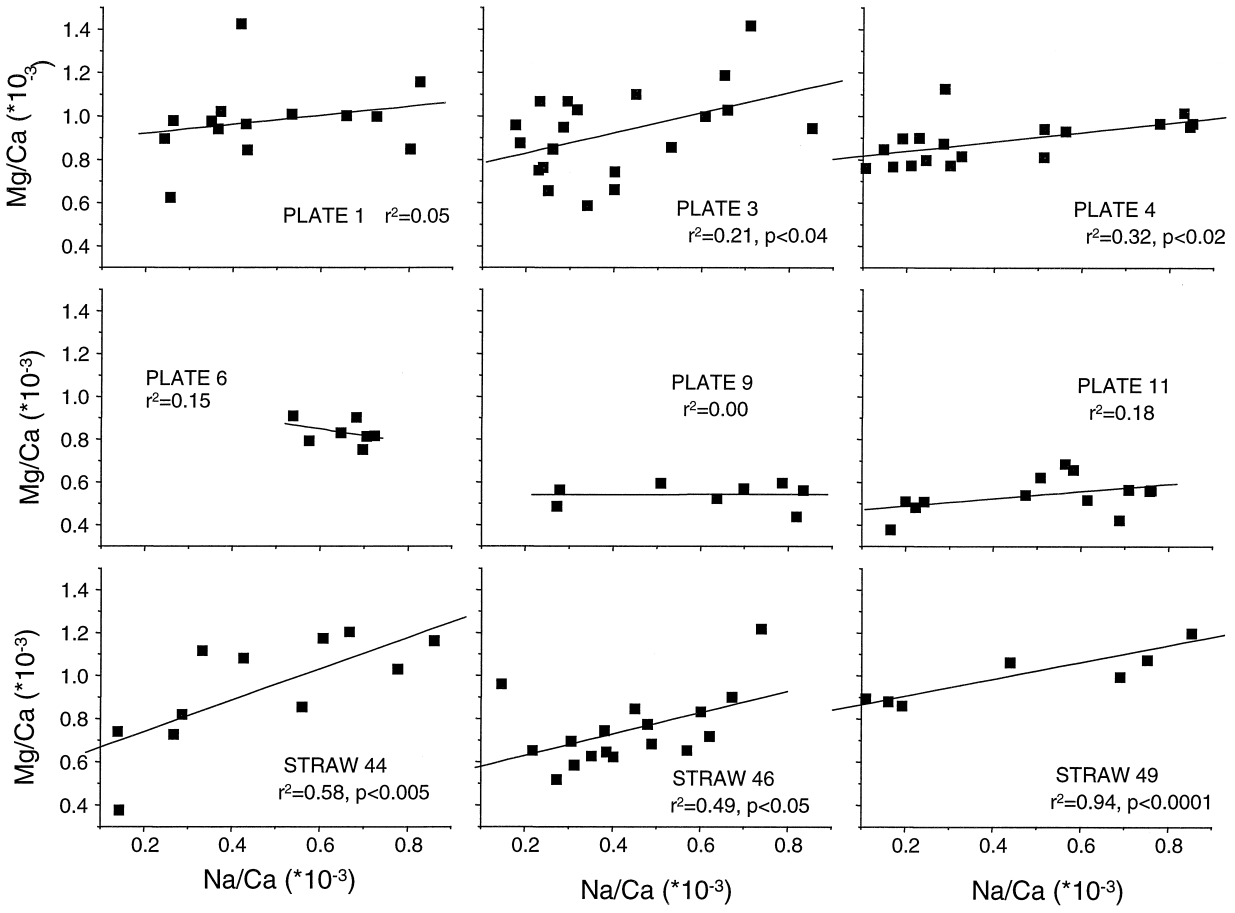

Fig. 7. Mg/Ca versus Na/Ca plot of the different measurements of each sample. Each point represents the mean of the later analytical cycles on the analytical spot on a given crystal.

field-based data (mean 0.014) of Huang et al. (2000) from a cave at 6.6°C with low Mg/Ca. Our best estimate of the temperature-sensitivity of D_{Mg} in cave waters of low ionic strength is thus a rise of 0.0006 per °C from 6.6 to 15°C and of 0.0012 per °C from 15 to 25°C. The increase in gradient with temperature is consistent with other data of Figure 11 obtained under different experimental conditions.

4.4. Application to Natural Environments

The prime motivation for the experimental studies was to apply the results to those natural environments where calcite precipitates from low ionic strength solutions. We will discuss the implications firstly in relation to the hydrodynamic environment of precipitation and secondly for crystal growth phenomena, before moving on to the application of Mg and Sr partition coefficients.

The experiments were set up to mimic geometrically the thin film environment of speleothem precipitation with a typical slow rate of movement of water through a tube (straw), falling at intervals as drops which splash onto a surface (plate) below. There are no systematic differences in the trace element partitioning behaviour of straws and plates, whose growth rates are also very similar. This demonstrates no over-riding control on elemental partitioning by the dynamics of water movement at the site of precipitation and hence we predict no differences between calcites forming from meteoric waters as a function of their geometric position. A future programme should attempt to demonstrate that this is so even if degassing of an initially CO_2-oversaturated solution occurs, although it will be more difficult to establish an experimental protocol whereby growth rates could be controlled under such conditions.

Previous experimental studies have used bulk analyses and so have not been designed to test for microscopic inhomogeneities in calcite composition resulting from the intrasectoral zoning phenomenon of Paquette and Reeder (1995). Our experiments clearly demonstrate differences in trace element composition between adjacent experimental crystals grown under identical conditions. Since the compositional variation is antipathetic for Sr and Mg and the mean composition of experimental products is similar for experiments under the same conditions, we attribute this spread to the analysis of intrasectorally zoned crystals. The analytical points are interpreted to have intersected different proportions of two types of vicinal faces around putative growth hillocks on the rhombohedral growth surfaces of such crystals. Any series of micro-analyses of calcite in which antipathetic variation of Sr and Mg is found would therefore need to be scrutinized with this phenomenon in mind. For example, Roberts et al. (1998) demonstrated antipa-

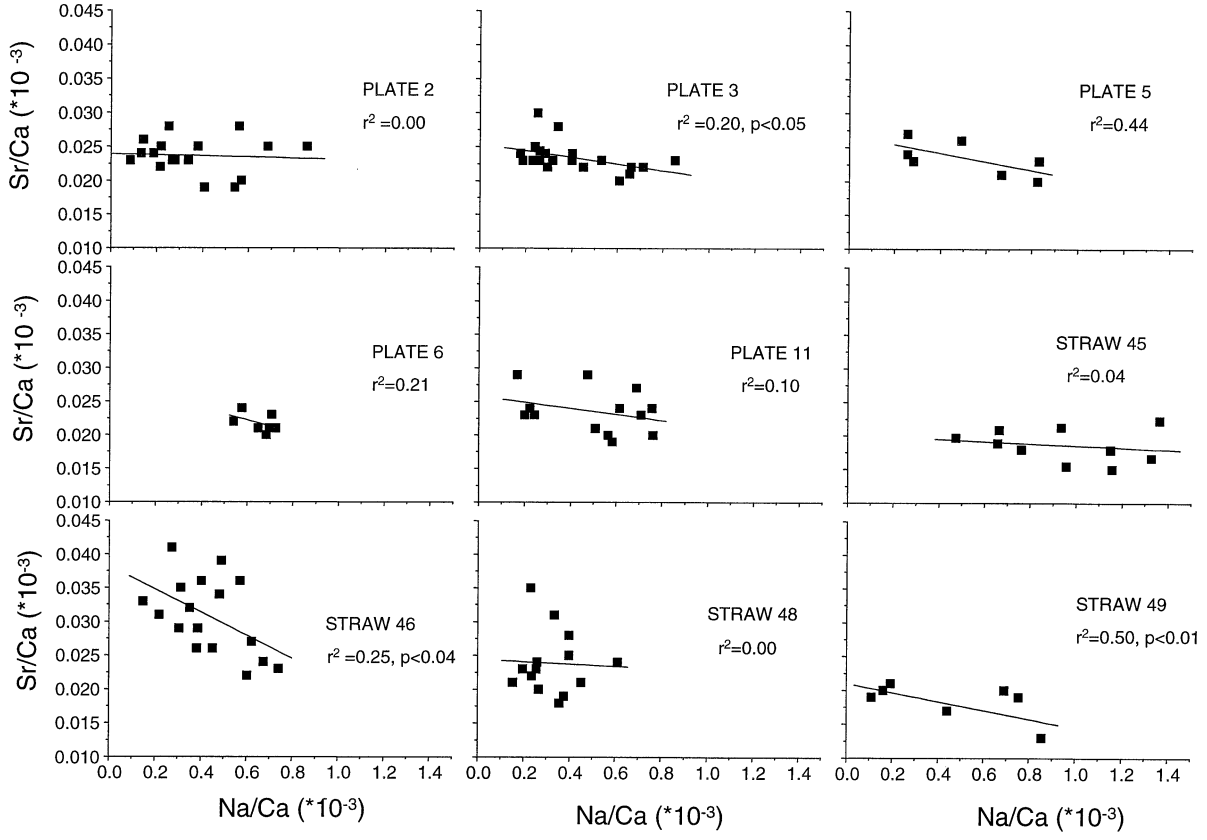

Fig. 8. Sr/Ca versus Na/Ca plot as Figure 7.

thetic annual variation in Sr and Mg from a Scottish speleothem. However it seems clear that intrasectoral zonation was not responsible for such variations since the latter coincided with the development of annual UV fluorescent laminae and the variations were shown to be continuous parallel to the fluorescing laminae. Other published ion microprobe work by Huang et al. (2000) shows sympathetic or uncorrelated Mg-Sr variation. This implies that, in all these cases, either inhomo-

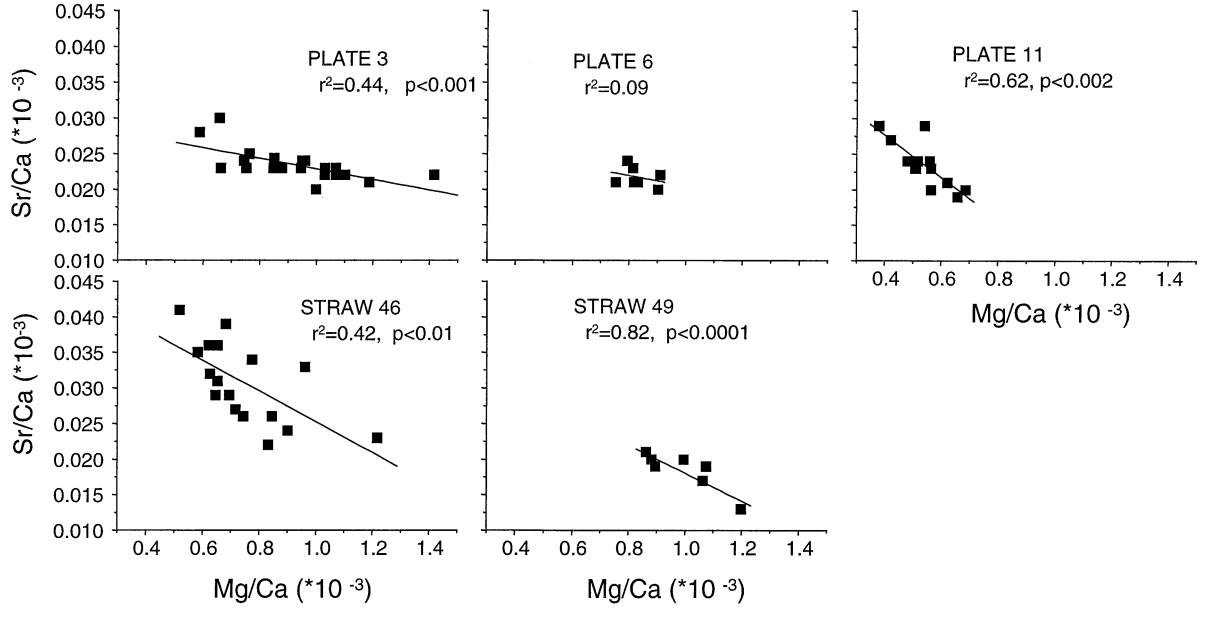

Fig. 9. Sr/Ca versus Mg/Ca plot as Figure 7.

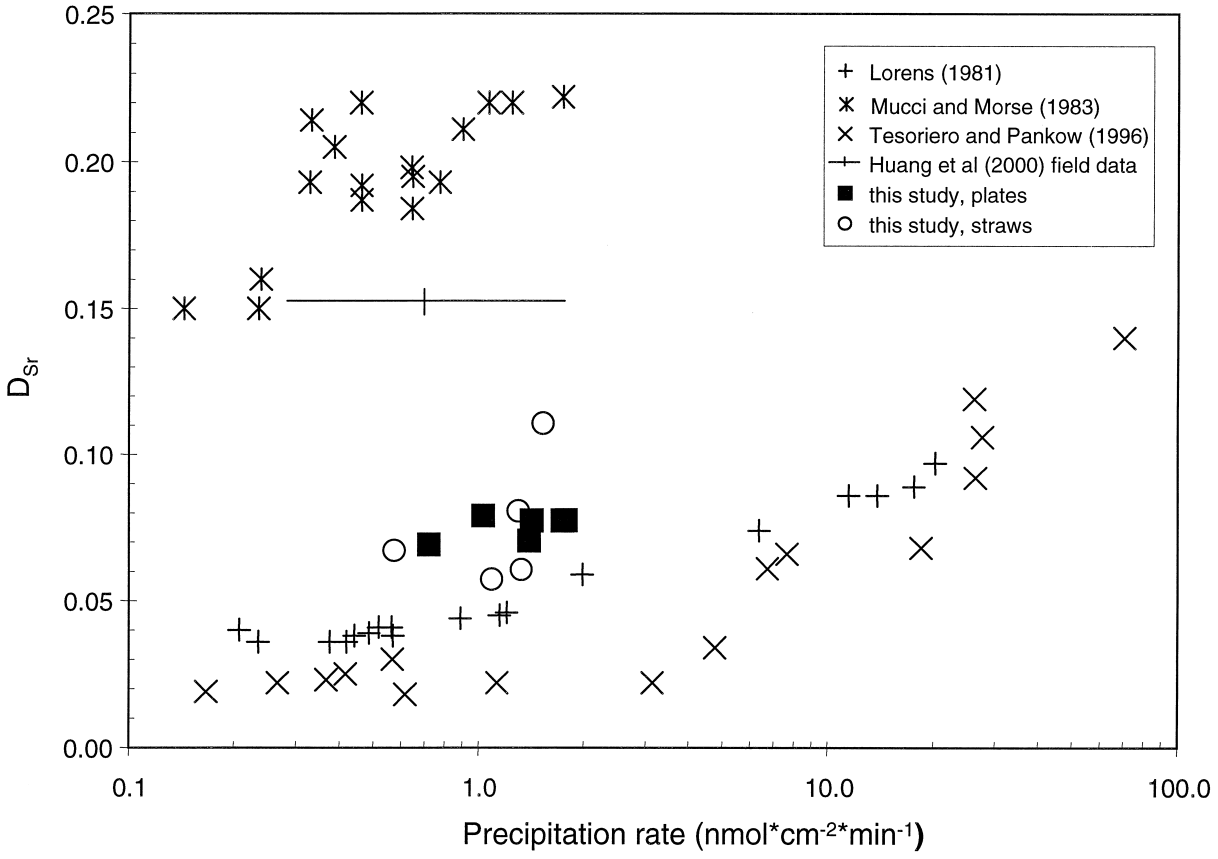

Fig. 10. D_{Sr} versus precipitation rate from the present study in comparison with previous work. The D_{Sr} from field data from Huang et al. (2000), consistent with other field data mentioned in the introduction, are also plotted for comparison. Lorens; 1981 used aqueous Sr/Ca = 0.00003, $PCO_2 = 10^{-2}$ and $CaCl_2$-$NaHCO_3$ solutions in 0.69 mol/L NaCl. Mucci and Morse (1983) used artificial and aged natural seawater (results for Mg/Ca = 1 are plotted), aqueous Sr/Ca = 0.042 and $PCO_2 = 10^{-2.5}$. Tesoriero and Pankow (1996) used $CaCl_2$-$NaCO_3$ solutions with 0.22 mol/L NaCl, Sr.Ca = 0.055 to 0.117 and $PCO_2 = 10^0$. All authors used heterogeneous nucleation from solutions of constant composition at 25°C.

geneities related to any growth hillocks are averaged out on the scale of analysis, or hillocks were not developed. Future micro-analyses of natural speleothems should bear this issue in mind and TEM studies of experimental and natural calcites are recommended to improve our general understanding of this phenomenon.

The 25°C result of the new experiments is consistent with the results of Howson et al. (1987), who showed that D_{Mg} is constant up to an Mg/Ca ratio of 1. This range covers the vast majority of karstic and other freshwater environments, whereas D_{Mg} would be somewhat lower at higher Mg/Ca ratios. Our results for the temperature-sensitivity for D_{Mg} is intermediate between that of experimental studies on marine-analog solutions and that deduced by Gascoyne (1983) from comparison of caves at two different temperatures. The approach of Gascoyne (1983) had a flaw in that bulk analyses of speleothems were used, hence concealing any subannual variations that are now known to be common, whereas the water analyses were only based on part of a year. Hence we consider that our result is more robust.

The knowledge of temperature sensitivity could be applied in future to annually-banded tufas to determine variations in stream temperatures. By contrast, in cave interiors, temperature is constant over time periods of up to decades and hence varying Mg content of speleothems will directly track varying solution Mg/Ca. In the study referred to above by Roberts et al. (1998), analyses were based on a speleothem near a cave entrance in which significant annual temperature variations could not be excluded. However, our result vindicates their conclusion that temperature variations were quantitatively insufficient to account for the annual changes in speleothem Mg content and hence that the Mg/Ca ratio of dripwater must have varied.

There have been several tests of the suggestion of Gascoyne (1983) that long-term variation in temperature might be determined by analysis of Mg (or Mg/Sr) in speleothems. Gascoyne (1992), Goede (1994) and Roberts et al. (1999) clearly demonstrated that the inadequacy of this approach, indicating changes in Mg/Ca and Mg/Sr of cave waters over time must have occurred. Fairchild et al. (2000) and Tooth (2000) have related cave water compositions to that of contributing bedrocks and demonstrated changes in space and over time which indicate that variations in speleothems should be dominated by the change of dripwater composition, which in turn reflects water availability in the karst zone. The variations in compositions of water, and hence of speleothems, are large compared

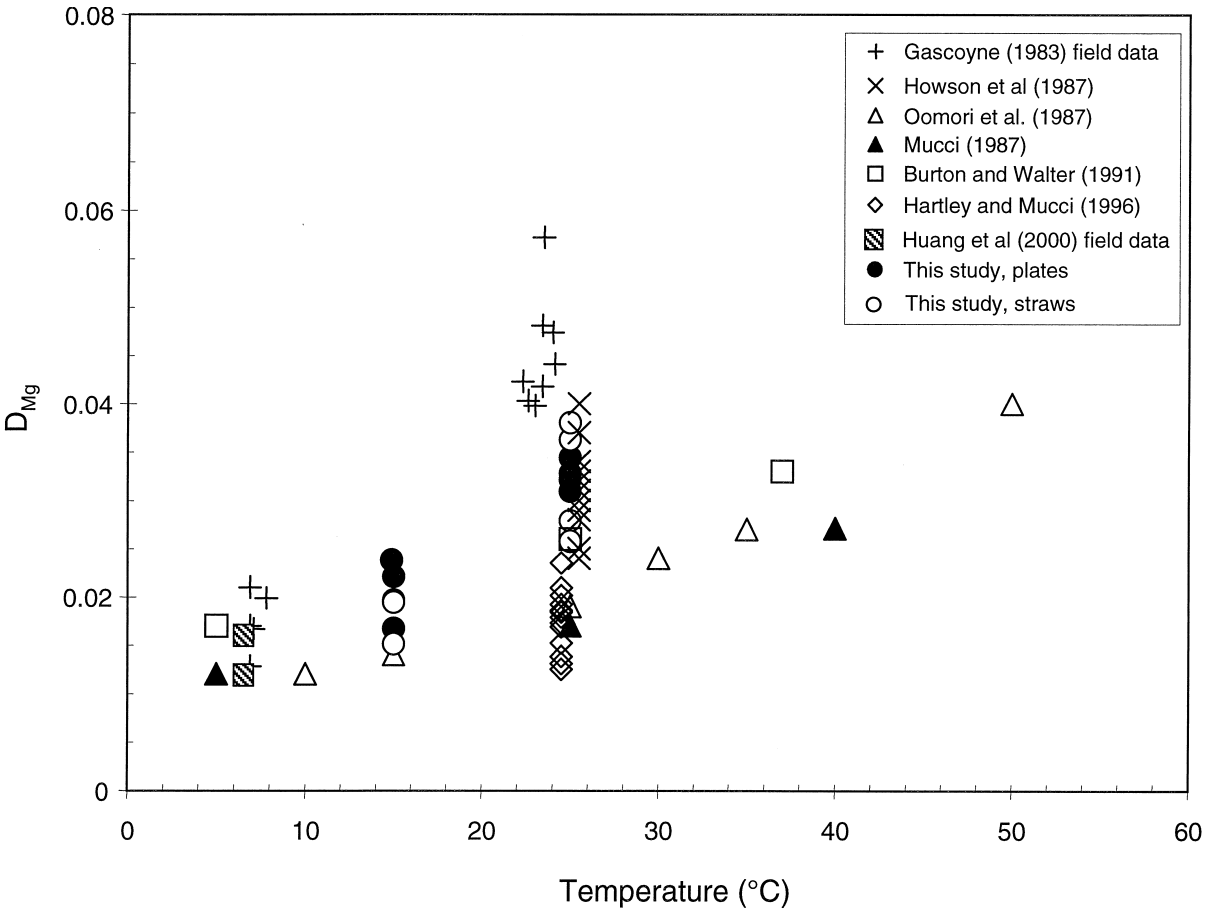

Fig. 11. D_{Mg} determinations (mean and standard deviation) versus temperature from experiments and cave data. The 25°C data are offset slightly from each other slightly for clarity. Howson et al. (1987), (see also House et al., 1988) used Ca-Mg-HCO_3 solutions with Mg/Ca in the range 0.15 to 1 and with a PCO_2 of $10^{-2.3}$ to $10^{-1.9}$. Oomori et al. (1987) used Ca-Mg-HCO_3 solutions with Mg/Ca in the range 0.04 to 2, but PCO_2 was uncontrolled (homogeneous nucleation during rapid degassing). The Mucci (1987) data (see also Mucci and Morse, 1983) are a subset of their whole dataset and used artificial seawater, with Mg/Ca modified to unity with PCO_2 of $10^{-2.5}$. Data plotted from Burton and Walter (1991) are from that subset of their results which used $MgCl_2$-$CaCl_2$ solutions with Mg/Ca = 5 and at PCO_2 of $10^{-3.5}$. Hartley and Mucci (1996) used artificial sea water with PCO_2 varying from 10^{-5} to $100^{-0.53}$. The field data of Huang et al. (2000), 0.016 and 0.012 at 6.6°C, are based on comparison of: a) mean ion microprobe data on laminae forming during recent decades in a stalagmite and a stalactite respectively with b) mean water data representing repeated sampling at different seasons during a 3 yr period in a cave in northern Italy. The field data of Gascoyne (1983) are from Vancouver Island and Jamaica. They are less reliable as they refer to a comparison of surface speleothem (assumed to be modern) and water from a single episode of sampling.

with potential changes in speleothem composition resulting from temperature variations in D_{Mg}. Our work indicates that for high resolution studies of speleothems from cave interiors, D_{Mg} will be constant and so speleothem Mg contents will directly track solution Mg/Ca ratios and hence palaeohydrology.

Our results for D_{Sr} are intermediate between the high values typical of Mg-calcites and the low values in Na-rich solutions from previous studies. However, they are still only around half the value of 0.15 deduced from previous studies in caves, including that of Huang et al. (2000) based on micro-analyses from cave precipitates at similar annual growth rates and low Sr/Ca ratios as our experiments. The factor of two uncertainty in the partition coefficient and its dependence on growth rate means that variations in Sr abundance need to interpreted more cautiously than in the case of Mg.

We distinguish two interpretable situations: 1) where the variation in Sr can be argued to reflect a change in Sr composition in the precipitating solution (which may relate to palaeoclimate); and 2) where the subannual variation in the speleothem may reflect growth rate or other crystallographic effects (for example related to the seasonality of cave water chemistry).

Goede et al. (1998) and Ayalon et al. (1999) found a bimodal distribution of Sr abundances, corresponding to glacial and interglacial growth layers of speleothems. Differences in Sr isotope composition between these sample groups allowed these authors to deduce that there was a change in Sr sourcing corresponding to major climatic shifts, with more exogenic Sr resulting from enhanced wind activity in glacial periods. The fact that Sr abundances displayed less than a factor of two

variation throughout, implies a relatively constancy of D_{Sr} values. Another case where the uncertainty in D_{Sr} is unimportant arises where solution Sr/Ca ratios show large variations over time. For example, Baker et al. (in press) found an order of magnitude increase in Sr/Ca in dripwaters in late summer related to hydrological changes during dry conditions in a French Jurassic limestone aquifer. We would deduce that speleothems forming from such dripwaters would display similarly large annual variations and hence would directly record hydrological conditions.

The variation in D_{Sr} with crystal chemical factors becomes more important where solution Sr/Ca shows little variation over time. However, the circumstances are restricted such that only small variations in Sr content of speleothems could be explained entirely in terms of changing growth rates. Variations of growth rate of around an order of magnitude would lead to changes in D_{Sr} of around 15%, based on the experimental studies illustrated in Figure 9. However, such substantial and sustained growth rate variations are not predicted from cave water chemistry studies (Baker et al. 1998) except that growth may cease entirely if dripwater supply abates. Huang et al. (2000) describe such a case where an annual variation in Sr/Ca of around 30% is much greater than that in repeated samples of the corresponding dripwater and where growth rates effects can be implicated. However, it is also possible that other crystallographic factors were involved. At the same site, Frisia et al. (2000) demonstrated seasonal variations in the morphology of crystallites forming on glass slides placed under dripwaters. The surfaces of the winter and spring crystallites are rough and have a high density of macro steps, visible at corners or edges whereas the crystallites that formed during summer and autumn are smaller in size and rhombohedral, exhibiting flat faces, with growth steps noticeable mainly on the smaller crystals. Therefore a combination of variation in growth rate per se and associated style of growth could be largely responsible for much of the annual Sr variation in the speleothem. More generally we would suggest that where patterns of covariation of Mg and Sr in modern speleothems differ from those of Mg/Ca and Sr/Ca in corresponding dripwaters, these variations could be related to growth rate modulation of D_{Sr}.

5. CONCLUSIONS

A new experimental system to mimic the conditions of calcite crystal growth from water films in natural karst caves has been successfully employed. Crystals up to 100 μm in size were grown over periods of 6 weeks, at temperatures of 15 and 25°C, with the addition of trace quantities of Mg and Sr to a $CaCl_2$-$NaHCO_3$ solution of low ionic strength. No consistent differences in morphology or chemistry were seen between "stalactite" and "stalagmite" growth situations. Individual 20 μm analytical spots from different crystals in the same experiment display variation in Sr that is inverse to that of Na and Mg. This is attributed to the occurrence of growth hillocks associated with differential trace element incorporation in vicinal faces. Such phenomena have not been encountered so far in ion probe studies on natural speleothems implying that any growth hillocks are on a finer spatial scale.

Mean values of D_{Mg} are 0.031 at 25°C, dropping to 0.019 at 15°C. The slope of this temperature-related variation is consistent with a cave value of 0.012 at 6.6°C. No other factors are thought to influence Mg partitioning in low ionic strength, low Mg/Ca solutions. The data enable prediction of fluctuations in Mg incorporation in freshwater calcites where annual temperature fluctuations are known. In most common cave environments where cave is relatively isothermal, effect of temperature on Mg/Ca ratio in speleothem is much smaller than Mg variation in cave waters, Mg variation can be reliably linked to solution composition, which recent work suggests is related to water availability in the karstic system.

Mean values of D_{Sr} are intermediate between the high values of Mg-rich solutions and low values obtained in Na-rich solutions. There is the suggestion of a positive relationship with growth rate, but growth rate was not varied over a wide-enough range to find a statistically-significant relationship. Variations in growth rate, if more than an order of magnitude, may play a role in the evolution of freshwater calcite composition, but in caves change in solution Sr/Ca, often found in parallel with Mg/Ca variations, can be a more powerful agent. We have reduced the discrepancy between experimental and field estimates of D_{Sr}, but there is a remaining uncertainty that may relate to a combination of crystal growth mechanism and varying short-term speleothem growth rates.

Acknowledgments—This work was supported by NERC grant GR3/10801. Ion microprobe analyses were carried out at the national facility at the University of Edinburgh, where Richard Hinton and John Craven gave invaluable assistance. Technical advice on the experiments from Professor Brigid Heywood (School of Chemistry and Physics, University of Keele) and technical support from Ian Wilshaw is gratefully acknowledged. Valuable suggestions for improvement of the manuscript were made by referees Elizabeth Burton and Jay Banner.

Associate editor: L. M. Walter

REFERENCES

Appelo C. A. J. and Postma D. (1994) Groundwater, Geochemistry and Pollution. A. A. Balkema, Rotterdam.

Ayalon A., Bar-Matthew M., and Kaufman A. (1999) Petrography, strontium, barium and uranium concentrations, and strontium and uranium isotope ratios in speleothems as paleoclimate proxies: Soreq cave, Israel. *The Holocene* **9,** 715–722.

Baker A., Genty D., Dreybrodt W., Barnes W. L., Mockler N. J., and Grapes J. (1998) Testing theoretically predicted stalagmite growth rate with Recent annually laminated samples: Implications for past stalagmite deposition. *Geochim. Cosmochim. Acta* **62,** 393–404.

Baker A., Genty D., and Fairchild I. J. (in press) Hydrological characterisation of stalagmite drip waters at Grotte de Villars, Dordogne, by the analysis of inorganic species and luminescent organic matter. *Hydr. Earth Sys. Sci.* (in press).

Banner J. L. (1995) Application of the trace element and isotope geochemistry of strontium to studies of carbonate diagenesis. *Sedimentology* **42,** 805–824.

Banner J. L., Musgrove M. L., Asmerom Y., Edwards R. L., and Hoff J. A. (1996) High-resolution temporal record of Holocene groundwater chemistry: Tracing links between climate and hydrology. *Geology* **24,** 1049–1053.

Bar-Matthews M., Ayalon A., Matthews A., Sass E., and Halicz, L. (1996) Carbon and oxygen isotope study of the active water-carbonate system in a karstic Mediterranean cave: Implications for paleoclimate research in semiarid regions. *Geochim. Cosmochim. Acta* **60,** 337–347.

Bar-Matthews M., Ayalon A., and Kaufman A. (1999) The Eastern Mediterranean paleoclimate as a reflection of regional events: Soreq cave, Israel. *Earth Planet. Sci. Lett.* **166,** 85–95.

Buhmann D. and Dreybrodt W. (1985) The kinetics of calcite disso-

lution and precipitation in geologically relevant situations of karst area. 1. Open System. *Chem. Geol.* **48,** 189–211.

Burton E. A. and Walter L. M. (1991) The effects of P_{CO2} and temperature on magnesium incorporation in calcite in seawater and $MgCl_2$-$CaCl_2$ solutions. *Geochim. Cosmochim. Acta* **55,** 777–785.

Busenberg E. and Plummer L. N. (1985) Kinetic and thermodynamic factors controlling the distribution of SO_4^{2-} and Na^+ in calcites and selected aragonites. *Geochim. Cosmochim. Acta* **49,** 713–725.

Fairchild I. J., Killawee J. A., Spiro B., and Tison J.-L. (1996) Calcite precipitates formed by freezing processes: Kinetic controls on morphology and geochemistry. In: *Proceedings of the fourth International Symposium on the Geochemistry of the Earth's Surface, Ilkley, Yorkshire, July 1996,* (ed. S. Bottrell) pp. 178–183, J. Wiley.

Fairchild I. J., Borsato A., Tooth A. F., Frisia S., Hawkesworth C. J., Huang Y., McDermott F., and Spiro B. (2000). Controls on trace element (Sr-Mg) compositions of carbonate cave waters: Implications for speleothem climatic records. *Chem. Geol.* **166,** 255–269.

Frisia S., Borsato A., Fairchild I. J., and McDermott F. (2000). Calcite fabrics, growth mechanisms and environments of formation in speleothems (Italian Alps and SW Ireland), *J. Sed. Res.* (in press).

Gascoyne M. (1983) Trace element partition coefficients in the calcite-water system and their palaeoclimatic significance in cave studies. *J. Hydrol.* **61,** 213–222.

Gascoyne M. (1992) Palaeoclimate determination from cave calcite deposits. *Quat. Sci. Rev.* **11,** 609–632.

Goede A. (1994) Continuous early last glacial palaeoenvironmental record from a Tasmanian speleothem based on stable isotope and minor element variations. *Quat. Sci Rev.* **13,** 283–291.

Goede A., McCulloch M., McDermott F., and Hawkesworth C. (1998) Aeolian contribution to strontium and strontium isotope variations in a Tasmanian speleothem. *Chem. Geol.* **149,** 37–50.

Hart S. R. and Cohen A. L. (1996) An ion probe study of annual cycles of Sr/Ca and other trace elements in corals. *Geochim. Cosmochim. Acta* **60,** 3075–3084.

Hartley G. and Mucci A. (1996) The influence of PCO_2 on the partitioning of magnesium in calcite overgrowths precipitated from artificial seawater at 25 degrees and 1 atm total pressure. *Geochim. Cosmochim. Acta* **60,** 315–324.

Holland H. D., Kirsipu T. V., Huebner J. S., and Oxburgh U. M. (1964) On some aspects of the chemical evolution of cave waters. *J. Geol.* **72,** 36–67.

House W. A., Howson M. R., and Pethybridge A. D. (1988) Crystallization kinetics of calcite in the presence of magnesium ions. *J. Chem. Soc., Faraday Trans.* **84,** 2723–2734.

Howson M. R., Pethybridge A. D., and House W. A. (1987) Synthesis and distribution coefficient of low-magnesium calcites. *Chem. Geol.* **64,** 79–87.

Huang Y., Fairchild I. J., Borsato A., Frisia S., Cassidy N. J., McDermott F., and Hawkesworth C. J. (2000). Seasonal variations in Sr, Mg and P in modern speleothems (Grotta di Ernesto, Italy) *Chem. Geol.* (in press).

Ishikawa M. and Ichikuni M. (1984) Uptake of sodium and potassium by calcite. *Chem. Geol.* **42,** 137–146.

Katz A., Sass E., Starinsky A., and Holland H. D. (1972) Strontium behaviour in the aragonite-calcite transformation: An experimental study at 40–98°C and one atmosphere. *Geochim. Cosmochim. Acta* **37,** 1536–1586.

Kaufman A., Wasserburg G. J., Porcelli D., Bar-Matthews M., Ayalon A., and Halicz L. (1998) U-Th isotope systematics from the Soreq cave, Israel and climatic correlations. *Earth Planet. Sci. Lett.* **156,** 141–155.

Killawee J. A., Fairchild I. J., Tison J.-L., Janssens L., and Lorrain R. (1998) Segregation of solutes and gases in experimental freezing of dilute solutions: Implications for natural glacial systems. *Geochim. Cosmochim. Acta* **62,** 3637–3655.

Lorens R. B. (1981) Sr, Cd, Mn and Co distribution coefficients in calcite as a function of calcite precipitation rate. *Geochim. Cosmochim. Acta* **45,** 553–561.

Malone M. J. and Baker P. A. (1999) Temperature dependence of the strontium distribution coefficient in calcite: An experimental study from 40 to 200°C and application to natural diagnetic calcites. *J. Sed. Res.* **69,** 216–233.

McDermott F., Frisia S., Huang Y., Longinelli A., Spiro B., Heaton T. H. E., Hawkesworth C. J., Borsato A., Keppens E., Fairchild I. J., van der Borg K., Verheyden S., and Selmo E. (1999) Holocene climate variability in Europe: Evidence from $\delta^{18}O$ and textural variations in speleothems. *Quat. Sci. Rev.* **18,** 1021–1038.

McIntyre W. L. (1963) Trace element partition coefficients—a review of theory and application to geology. *Geochim. Cosmochim. Acta* **27,** 1209–1264.

Morse J. W. and Bender M. L. (1990) Partition coefficients in calcite: Examination of factors influencing the validity of experimental results and their application to natural systems. *Chem. Geol.* **82,** 265–277.

Mucci A. (1986) Growth kinetics and composition of magnesian calcite overgrowth precipitated from seawater: Quantitative influence of orthophosphate ions. *Geochim. Cosmochim. Acta* **50,** 2255–2265.

Mucci A. (1987) Influence of temperature on the composition of magnesian calcite overgrowths precipitation from seawater. *Geochim. Cosmochim. Acta.* **51,** 1977–1984.

Mucci A. and Morse J. W. (1983) The incorporation of Mg^{+2} and Sr^{+2} into calcite overgrowths: influences of growth rate and solution composition. *Geochim. Cosmochim. Acta* **47,** 217–233.

Mucci A. and Morse J. W. (1990) Chemistry of low-temperature abiotic calcites: Experimental studies on coprecipitation, stability and fractionation. *Rev. Aqu. Sci.* **3,** 217–254.

Nürnberg D., Bijma J., and Hemleben C. (1996) Assessing the reliability of magnesium in foraminiferal calcite as a proxy for water mass temperatures. *Geochim. Cosmochim. Acta* **60,** 803–814.

Oomori T., Kaneshima H., Maezato Y., and Kitano Y. (1987) Distribution coefficient of Mg^{2+} ions between calcite and solution at 10–50°C. *Mar. Chem.* **20,** 327–336.

Paquette J. and Reeder R. J. (1990) New type of compositional zoning in calcite: Insights into crystal-growth mechanisms. *Geology* **18,** 1244–1247.

Paquette J. and Reeder R. J. (1995) Relationship between surface structure, growth mechanism, and trace element incorporation in calcite. *Geochim. Cosmochim. Acta* **59,** 735–749.

Pingitore N. E. and Eastman M. P. (1986) The coprecipitation of Sr^{2+} with calcite at 25°C and 1 atmosphere. *Geochim. Cosmochim. Acta* **50,** 2195–2203.

Pingitore N. E., Lyttle F. W., Davies B. M., Eastman M. P., Eller P. G., and Larson E. M. (1992) Model of incorporation of Sr^{2+} in calcite: Determination by X-ray absorption spectroscopy. *Geochim. Cosmochim. Acta* **56,** 1531–1538.

Reeder R. J. (1996) Interaction of divalent cobalt, zinc, cadmium, and barium with the calcite surface during layer growth. *Geochim. Cosmochim. Acta* **60,** 1543–1552.

Reeder R. J. and Grams J. C. (1987) Sector zoning in calcite cement crystals: Implications for trace element distributions in carbonates. *Geochim. Cosmochim. Acta* **51,** 187–194.

Reeder R. J., Lamble G. M., and Northrup P. A. (1999) XAFS study of the coordination and local relaxation around Co^{2+}, Zn^{2+}, Pb^{2+}, and Ba^{2+} trace elements in calcite. *Am. Miner.* **84,** 1049–1060.

Roberts M. S., Smart P. L., and Baker A. (1998) Annual trace element variations in a Holocene speleothem. *Earth Planet. Sci. Lett.* **154,** 237–246.

Roberts M. S., Smart P. L., Hawkesworth C. J., Perkins W. T., and Pearce N. J. G. (1999) Trace element variations in coeval Holocene speleothems from GB Cave, southwest England. *The Holocene* **9,** 707–713.

Shiraki R. and Brantley S. L. (1995) Kinetics of near-equilibrium calcite precipitation at 100°C, an evaluation of elementary reaction-based and affinity-based rate laws. *Geochim. Cosmochim. Acta* **59,** 1457–1471.

Staudt W. J., Reeder R., and Schoonen M. A. A. (1994) Surface structural controls on compositional zoning of SO_4^{2-} and SeO_4^{2-} in synthetic calcite single crystals. *Geochim. Cosmochim. Acta* **58,** 2087–2098.

Teng H. H., Dove P. M. and DeYoreo J. J. (1999) Reversed calcite morphologies induced by microscopic growth kinetics: Insight into biomineralization. *Geochim. Cosmochim. Acta* **63,** 2507–2512.

Tesoriero A. J. and Pankow J. F. (1996) Solid solution partitioning of Sr^{2+}, Ba^{2+} and Cd^{2+} into calcite. *Geochim. Cosmochim. Acta* **60,** 1053–1063.

Tooth A. F. (2000). The evolution of the geochemical signal of speleothem-forming karstic drip waters. Unpubl. Ph.D. thesis, Keele U.

Veizer J. (1983) Chemical diagenesis of carbonates: theory and application of trace element technique. In: *Stable Isotopes in Sedimentary Geology* (eds. M. A. Arthur and T. F. Anderson), *Soc. Econ. Paleont. Mineral. Short Course* **10,** 3-1–3-100.

Xia J., Engstrom D. R., and Ito E. (1997) Geochemistry of ostracode calcite: Part 2. The effects of water chemistry and seasonal temperature variation on *Candona rawsoni*. *Geochim. Cosmochim. Acta* **61,** 383–391.

Zhong S. and Mucci A. (1989) Calcite and aragonite precipitation from seawater solutions of various salinities: Precipitation rates and overgrowth compositions. *Chem. Geol.* **78,** 283–299.